Synthesis and Applications of Low-Bandgap Conjugated Polymers Containing Phenothiazine Donor and Various Benzodiazole Acceptors for Polymer Solar Cells

HARIHARA PADHY,[1] JEN-HSIEN HUANG,[2] DURYODHAN SAHU,[1] DHANANJAYA PATRA,[1] DHANANJAY KEKUDA,[2] CHIH-WEI CHU,[2,3] HONG-CHEU LIN[1]

[1]Department of Materials Science and Engineering, National Chiao Tung University, Hsinchu, Taiwan, Republic of China

[2]Research Center for Applied Sciences, Academia Sinica, Taipei, Taiwan, Republic of China

[3]Department of Photonics, National Chiao Tung University, Hsinchu, Taiwan, Republic of China

Received 6 June 2010; accepted 15 July 2010
DOI: 10.1002/pola.24273
Published online 20 September 2010 in Wiley Online Library (wileyonlinelibrary.com).

ABSTRACT: A series of soluble donor-acceptor conjugated polymers comprising of phenothiazine donor and various benzodiazole acceptors (i.e., benzothiadiazole, benzoselenodiazole, and benzoxadiazole) sandwiched between hexyl-thiophene linkers were designed, synthesized, and used for the fabrication of polymer solar cells (PSC). The effects of the benzodiazole acceptors on the thermal, optical, electrochemical, and photovoltaic properties of these low-bandgap (LBG) polymers were investigated. These LBG polymers possessed large molecular weight (M_n) in the range of 3.85−5.13 × 10^4 with high thermal decomposition temperatures, which demonstrated broad absorption in the region of 300−750 nm with optical bandgaps of 1.80−1.93 eV. Both the HOMO energy level (−5.38 to −5.47 eV) and LUMO energy level (−3.47 to −3.60 eV) of the LBG polymers were within the desirable range of ideal energy level. Under 100 mW/cm^2 of AM 1.5 white-light illumination, bulk heterojunction PSC devices containing an active layer of electron donor polymers mixed with electron acceptor [6,6]-phenyl-C_{61}-butyric acid methyl ester ($PC_{61}BM$) or [6,6]-phenyl-C_{71}-butyric acid methyl ester ($PC_{71}BM$) in different weight ratios were investigated. The best performance of the PSC device was obtained by using polymer PP6DHTBT as an electron donor and $PC_{71}BM$ as an acceptor in the weight ratio of 1:4, and a power conversion efficiency value of 1.20%, an open-circuit voltage (V_{oc}) value of 0.75 V, a short-circuit current (J_{sc}) value of 4.60 mA/cm^2, and a fill factor (FF) value of 35.0% were achieved. © 2010 Wiley Periodicals, Inc. J Polym Sci Part A: Polym Chem 48: 4823–4834, 2010

KEYWORDS: conjugated polymers; copolymerization; donor-acceptor; heteroatom-containing polymers; phenothiazine derivatives; solar cells

INTRODUCTION Despite the poor long-term stability, polymer solar cell (PSC) devices based on conjugated polymers as electron donors and fullerene derivatives as electron acceptors are of broad interests because of the advantages of low cost, light-weight flexible devices, tunable electronic properties, and ease of processing for the conversion of solar energy to electricity.[1–7] Although poly(3-hexylthiophene) (P3HT) is proven to be one of the most efficient donor materials ever tested in PSCs for giving the power conversion efficiency (PCE) up to 5%,[2] further enhanced PCE values are limited because of both lower photocurrent generation and intrinsic absorption properties. To conquer these problems, low-bandgap (LBG) polymers composed of electron-rich (donor) and electron-deficient (acceptor) units have been utilized recently in PSCs with fullerene derivatives, such as [6,6]-phenyl-C_{61}-butyric acid methyl ester ($PC_{61}BM$) or [6,6]-phenyl-C_{71}-butyric acid methyl ester ($PC_{71}BM$), yielding a PCE value up to 7.7%.[3] PSCs consisting of such donor-acceptor (D-A) LBG polymers have attracted more attention owing to their tunable optical, electrochemical, electronic, and photovoltaic properties.[6] Incorporation of wide ranges of donors and acceptors into LBG polymers can manipulate the electronic structures, that is, the highest occupied molecular orbital (HOMO) and lowest unoccupied molecular orbital (LUMO) levels through the partial intramolecular charge transfer (ICT) in the D-A systems.[8] By optimizing materials and device structures, photovoltaic parameters, such as the short-circuit current (J_{sc}) and open-circuit voltage (V_{oc}), can be further improved to obtain higher PCE values in the PSCs. In solar cell devices, J_{sc} is determined by the creation and subsequent dissociation of excitons at the polymer/acceptor interface followed by transport of free charge carriers towards the collecting electrodes,[9] V_{oc} is primarily determined by the effective band gap of the bulk hetero-junction (BHJ) film.[7(a)] For this purpose, the electron donor polymer should exhibit a band gap between 1.2 and 1.9 eV, which

Correspondence to: H.-C. Lin (E-mail: linhc@cc.nctu.edu.tw)
Journal of Polymer Science: Part A: Polymer Chemistry, Vol. 48, 4823–4834 (2010)

corresponds to a HOMO energy level between −5.8 and −5.2 eV and a LUMO energy level between −4.0 and −3.8 eV.[1(c)] Again, if the energy difference between the LUMO levels of polymer and acceptor is less than 0.3 eV,[10] the driving force for charge separation will be reduced, and V_{oc} can be reduced by raising the HOMO level. Consequently, it is of great importance to match the energy levels of the polymer and acceptor carefully to develop BHJ solar cells with high efficiencies.

Among all heterocyclic compounds, phenothiazine contains both electron-rich sulfur and nitrogen heteroatoms. The electron-rich nature of phenothiazine contributes for the efficient electron donor and hole transporting materials in polymers and organic molecules for photo-induced charge separation and it has been also proven as a superior electron donor for reductive quenching.[11] Because of their unique electro-optical properties, these materials are potential candidates for diverse applications for light-emitting diodes,[12] solar cells, chemiluminescence devices,[13] and organic field effect transistors.[12(b),14] Phenothiazine ring hampers stacking aggregation and intermolecular excimer formation in the main chain of the polymer due to its nonplanar structure.[15] However, till now only a limited number of phenothiazine-based polymers for photovoltaic devices have been explored.[16]

Addition of electron-withdrawing imine nitrogen to a conjugated polymer backbone generally enhances its electron-accepting properties and makes it susceptible to *n*-doping (reduction). Benzodiazole units are, in that sense, typical examples of such units containing imine nitrogen.[6(d)] 2,1,3-Benzothiadiazole is a widely used electron acceptor for the synthesis of D-A polymers. For example, copolymers of benzothiadiazole with fluorene,[17] silafluorene,[18] carbazole,[19] dithienosilole,[20] dithienocyclopentadiene,[21] and dithieno[3,2-b:2′,3′-d]pyrroles[22] were synthesized and applied to PSCs, yielding PCE values in the range of 0.18−5.4%. Recently, many photovoltaic papers have reported LBG copolymers made of electron donors and acceptors sandwiched between two thiophene units.[17–23] Incorporation of acceptor units in the midst of two thiophene units, alleviate the severe steric hindrance between the electron donors and acceptors, resulting in more planar structures to facilitate interchain associations and improve the hole mobilities of the LBG polymers. Despite these advantages, addition of thiophene units could induce solubility problems and yield low molecular weights in polymers.[17(a)] To utilize the aforementioned merits of thiophene units, structural modifications, such as incorporation of alkyl or alkoxy chains on the 3- and/or 4-position of thienyl units[17(c)] or addition of supplementary alkylated thiophene units,[17(d)] have been outfitted to acquire higher molecular weights and better solubilities than the original polymers without any soluble side-chains.

To have better photophysical, electrochemical, and photovoltaic properties in the resulting LBG polymers, the incorporation of phenothiazine donor units with various acceptor units are very intriguing and thus to motivate this study. Herein, we report the design, synthesis, properties, and device applications of phenothiazine-based alternating conjugated D-A polymers, in which the acceptor benzodiazole units include benzothiadiazole, benzoselenodiazole, and benzoxadiazole sandwiched between two hexyl thiophene units. These polymers were synthesized by palladium (0)-catalyzed Suzuki coupling reactions. The effects of D-A strengths on the electronic and optoelectronic properties of the LBG polymers were also investigated. In addition, the PSC devices fabricated by polymer/$PC_{61}BM$ or polymer/$PC_{71}BM$ blends sandwiched between a transparent anode (ITO/PEDOT:PSS) and a cathode (Ca) were explored.

EXPERIMENTAL

Materials

All chemicals and solvents were reagent grades and purchased from Aldrich, ACROS, Fluka, TCI, TEDIA, and Lancaster Chemical Co. Toluene, tetrahydrofuran, and diethyl ether were distilled over sodium/benzophenone to keep anhydrous before use. Chloroform ($CHCl_3$) was purified by refluxing with calcium hydride and then distilled. If not otherwise specified, the other solvents were degassed by nitrogen 1 h prior to use.

Measurements and Characterization

^{1}H-NMR and ^{13}C-NMR spectra were recorded on a Varian Unity 300 MHz spectrometer using $CDCl_3$ solvent. Elemental analyses were performed on a HERAEUS CHN-OS RAPID elemental analyzer. Thermogravimetric analyses (TGA) were conducted with a TA Instruments Q500 at a heating rate of 10 °C/min under nitrogen. The molecular weights of polymers were measured by gel permeation chromatography (GPC) using Waters 1515 separation module (concentration = 1 mg/mL in THF; flow rate = 1 mL/min), and polystyrene was used as a standard with THF as an eluant. UV−visible absorption spectra were recorded in dilute chlorobenzene solutions (10^{-5} M) and on solid films (spin-coated with a spin rate ∼1000 rpm for 60 s on glass substrates from chlorobenzene solutions with a concentration of 10 mg/mL) on a HP G1103A. Cyclic voltammetry (CV) measurements were performed using a BAS 100 electrochemical analyzer with a standard three-electrode electrochemical cell in a 0.1-M solution of tetrabutylammonium hexafluorophosphate ($(TBA)PF_6$) in acetonitrile at room temperature with a scanning rate of 100 mV/s. During the CV measurements, the solutions were purged with nitrogen for 30 s. In each case, a carbon working electrode coated with a thin layer of polymers, a platinum wire as the counter electrode, and a silver wire as the quasi-reference electrode were used, and Ag/AgCl (3 M KCl) electrode was served as a reference electrode for all potentials quoted herein. The redox couple of ferrocene/ferrocenium ion (Fc/Fc^+) was used as an external standard. The corresponding HOMO and LUMO levels were calculated using $E_{ox/onset}$ and $E_{red/onset}$ for experiments in solid films of polymers, which were performed by drop-casting films with the similar thickness from THF solutions (∼5 mg/mL). The onset potentials were determined from the intersections of two tangents drawn at the rising currents and background currents of the cyclic voltammetry (CV) measurements. Surface morphology images of thin films (on

glass substrates) were obtained using atomic force microscopy (AFM, Digital instrument NS 3a controller with D3100 stage).

Device Fabrication and Characterization of PSCs

The PSCs in this study were composed of an active layer of blended polymers (Polymer: PCBM) in solid films, which was sandwiched between a transparent indium tin oxide (ITO) anode and a metal cathode (Ca). Prior to the device fabrication, ITO-coated glass substrates (1.5 × 1.5 cm^2) were ultrasonically cleaned in detergent, deionized water, acetone, and isopropyl alcohol. After routine solvent cleaning, the substrates were treated with UV ozone for 15 min. Then a modified ITO surface was obtained by spin-coating a layer of poly(ethylene dioxythiophene): polystyrenesulfonate (PEDOT:PSS) (∼30 nm). After baking at 130 °C for 1 h, the substrates were transferred to a nitrogen-filled glovebox. Then, on the top of PEDOT:PSS layer, an active layer was prepared by spin coating from blended solutions of polymers:$PC_{61}BM$ (with 1:1 w/w) and PP6DHTBT:$PC_{71}BM$ (with 1:1, 1:3, and 1:4 w/w) subsequently with a spin rate ∼1500 rpm for 60 s, and the thickness of the active layer was typically ∼80 nm. Initially, the blended solutions were prepared by dissolving both polymers and PCBM in 1,2-dichlorobenzene (20 mg/mL), followed by continuous stirring for 12 h at 50 °C. In the slow-growth approach, blended polymers in solid films were kept in the liquid phase after spin-coating by using the solvent with a high boiling point. Finally, a calcium layer (30 nm) and a subsequent aluminum layer (100 nm) were thermally evaporated through a shadow mask at a pressure below 6 × 10^{-6} Torr. The active area of the device was 0.12 cm^2. All PSC devices were prepared and measured under ambient conditions. The solar cell testing was done inside a glove box under simulated AM 1.5G irradiation (100 mW/cm^2) using a Xenon lamp based solar simulator (Thermal Oriel 1000W). The light intensity was calibrated by a mono-silicon photodiode with KG-5 color filter (Hamamatsu). The external quantum efficiency (EQE) action spectrum was obtained at short-circuit condition. The light source was a 450 W Xe lamp (Oriel Instrument, model 6266) equipped with a water-based IR filter (Oriel Instrument, model 6123NS). The light output from the monochromator (Oriel Instrument, model 74100) was focused onto the photovoltaic cell under test.

Synthesis of Monomers and Polymers

General Synthetic Procedures for 4a–4c

In a 100-mL flame-dried two-neck flask fitted with a condenser, 1.00 equiv of dibromoarene (**3a–3c**), 2.2 equiv of 2-(4-hexylthiophen-2-yl)-4,4,5,5-tetramethyl-1,3,2-dioxaborolane (**2**), and 0.03 equiv of tetrakis (triphenylphosphine) palladium was added. The mixture was degassed and purged nitrogen. Afterward, 40 mL of anhydrous toluene and 2 M aqueous potassium carbonate solution (8 mL) was added. The reaction mixture was heated to 90 °C with vigorous stirring until reaction completion by TLC analyses (∼24 h). The mixture was poured into water (100 mL) and extracted with methylene chloride. The organic layer was washed thrice with water, once with brine and dried over magnesium sulfate. The solvent was evaporated and the residue was purified by column chromatography on silica gel with hexane/ethyl acetate = 20/1 to give the products. Their chemical characterization analyses are shown as follows:

4,7-Bis(4-hexylthiophen-2-yl)-2,1,3-benzothiadiazole (4a)

Orange needles (yield: 88%); mp 75–77 °C. ^{1}H-NMR (ppm, $CDCl_3$): δ 7.97 (dd, 2H), 7.82 (d, J = 1.8 Hz 2H), 7.04 (dd, 2H), 2.66 (t, J = 7.5 Hz, 4H), 1.70 (m, 4H), 1.25−1.53 (m, 12H), 0.90 (t, J = 6.7 Hz, 6H). ^{13}C-NMR (ppm, $CDCl_3$): δ 153.02, 139.75, 128.42, 127.90, 127.21, 126.38,126.15,. 31.68, 29.70, 29.65, 29.03, 22.67, 14.14.

4,7-Bis(4-hexylthiophen-2-yl)-2,1,3-benzoselenadiazole (4b)

Purple solid (yield: 87%); mp 82−83 °C. ^{1}H-NMR (ppm, $CDCl_3$): δ 7.87 (d, J = 1.2 Hz, 2H), 7.71 (s, 2H), 7.04 (d, J = 1.5 Hz, 2H), 2.68 (t, J = 7.8 Hz, 4H), 1.68 (m, 4H), 1.20−1.43 (m, 12H), 0.90 (t, J = 6.9 Hz, 6H). ^{13}C-NMR (ppm, $CDCl_3$): δ 158.19, 143.98, 139.29, 128.87, 127.42, 125.75,121.83,. 31.68, 30.56, 30.45, 29.04, 22.62, 14.10.

4,7-Bis(4-hexylthiophen-2-yl)-2,1,3-benzoxadiazole (4c)

Yellow solid (yield: 92%); mp 78−79 °C. ^{1}H-NMR (ppm, $CDCl_3$): δ 7.95 (d, J = 1.2 Hz, 2H), 7.57 (s, 2H), 7.02 (d, J = 1.2 Hz, 2H), 2.67 (t, J = 7.6 Hz, 4H), 1.70 (m, 4H), 1.20−1.43 (m, 12H), 0.89 (t, J = 7.2 Hz, 6H). ^{13}C-NMR (ppm, $CDCl_3$): δ 148.081, 145.28, 137.77, 30.40, 126.32, 122.31, 121.88, 31.90, 30.83, 30.65, 29.24, 22.85, 14.34.

General Bromination Procedures for 5a–5c

In a 100-mL flask, 1.00 equiv of 4,7-di(4-hexyl-2-thienyl)-arene (**4a**−**4c**) was added into THF under nitrogen flow. After solids were dissolved completely, 2.10 equiv *N*-bromosuccinimide (NBS) was added in portion wise. The reaction mixtures were stirred at a room temperature for 5 h. Subsequently, hexane was added into the mixture, and the white precipitate formed was filtered off. In addition, the filtrate was extracted with ethyl acetate, and the organic layer was washed with brine followed by being dried over anhydrous sodium sulfate. After that, the residue was purified by column chromatography on silica gel with hexane/methylene chloride = 1/2 to give the products. Their chemical characterization analyses are shown as follows:

4,7-Bis(5-bromo-4-hexyl-2-thienyl)-2,1,3-benzothiadiazole (5a)

Red solid (yield: 94%); mp 101−103 °C. ^{1}H-NMR (ppm, $CDCl_3$): δ 7.75 (s, 2H), 7.71 (s, 2H), 2.63 (t, J = 7.2 Hz, 4H), 1.67 (m, 4H), 1.33−1.40 (m, 12H), 0.89 (t, J = 7.1 Hz, 6H). ^{13}C-NMR (ppm, $CDCl_3$): δ 152.19, 143.01, 138.46, 128.03, 125.25, 124.80, 111.59, 31.62, 29.74, 29.67, 28.96, 22.64, 14.11. Element Anal. Calcd for $C_{26}H_{30}Br_2N_2S_3$: C, 49.84%; H, 4.83%; N, 4.47%; Found: C, 49.62%; H, 5.02%; N, 4.62%. EIMS (m/z): calcd for $C_{26}H_{30}$ $Br_2N_2S_3$, 626.53; found, 626.

4,7-Bis(5-bromo-4-hexyl-2-thienyl)-2,1,3-benzoselenadiazole (5b)

Purple solid (yield: 96%); mp 92−94 °C. ^{1}H-NMR (ppm, $CDCl_3$): δ 7.65 (s, 2H), 7.64 (s, 2H), 2.62 (t, J = 7.2 Hz, 4H), 1.67 (m, 4H), 1.33−1.42 (m, 12H), 0.90 (t, J = 6.9 Hz, 6H). (ppm, $CDCl_3$): δ 157.71, 142.62, 138.73, 127.63, 126.75, 124.93, 112.19, 31.62, 29.74, 29.67, 28.96, 22.64, 14.11.

Element Anal. Calcd for $C_{26}H_{30}Br_2N_2S_2Se$: C, 46.37%; H, 4.49%; N, 4.16. Found: C, 46.78%; H, 5.14%; N, 4.33%. EIMS (*m/z*): calcd for $C_{26}H_{30}$ $Br_2N_2S_3$, 673.43; found, 674.

4,7-Bis(5-bromo-4-hexyl-2-thienyl)-2,1,3- benzoxadiazole (5c)

Orange solid (yield: 93%); mp 108−110 °C. ^{1}H-NMR (ppm, $CDCl_3$): δ 7.77 (s, 2H), 7.38 (s, 2H), 2.60 (t, J = 7.2 Hz, 4H), 1.62 (m, 4H), 1.33−1.42 (m, 12H), 0.90 (t, J = 6.9 Hz, 6H). ^{13}C-NMR (ppm, $CDCl_3$): δ 147.42, 143.88, 137.08, 129.71, 125.68, 121.35, 111.56, 31.59, 29.66, 29.64, 28.94, 22.60, 14.10. Element Anal. Calcd for $C_{26}H_{30}Br_2N_2OS_2$: C, 51.15%; H, 4.95%; N, 4.59%. Found: C, 51.30%; H, 5.52%; N, 4.27%. EIMS (*m/z*): calcd for $C_{26}H_{30}$ $Br_2N_2S_3$, 610.47; found, 610.

10-Hexyl-3,7-bis(4,4,5,5-tetramethyl-1,3,2-dioxaborolan-2-yl)-10H-phenothiazine (7)

A solution of 3,7-dibromo-10-hexyl-10H-phenothiazine (4.41 g, 10 mmol) in anhydrous tetrahydrofuran (100 mL) was cooled to −78 °C under nitrogen and stirred at this temperature for 5 min in the flame-dried two-neck round-bottom flask. *n*-Butyl lithium (8.4 mL of 2.5 M solution in hexane, 21 mmol) was added dropwise, using a syringe, and the mixture was stirred at −78 °C, warmed to 0 °C for 15 min, and cooled again at −78 °C for 15 min. 2-Isopropoxy-4,4,5,5-tetramethyl-1,3,2-dioxaborolane (6.13 mL, 30 mmol) was added rapidly to the solution, and the resulting mixture was warmed to room temperature and stirred overnight. The mixture was poured into water and extracted with ether. The organic extracts were washed with brine and dried over magnesium sulfate. The solvent was removed by rotary evaporation, and the residue was recrystalized from acetone to obtain 3.96 g (74%) of the title product as a slight yellow solid ; mp 212−214 °C. ^{1}H-NMR (ppm, $CDCl_3$): δ 7.54 (m, 4H), 6.80 (d, J = 7.8 Hz, 2H), 3.84 (t, J = 6.9 Hz, 2H), 1.78 (m, 2H), 1.4 (m, 2H), 1.32 (s, 24H), 1.25 (m, 4H), 0.86 (t, J = 7.2 Hz, 3H). ^{13}C-NMR (ppm, $CDCl_3$): δ 147.47, 134.23, 133.97, 124.15, 114.90, 83.91, 47.71, 31.62, 26.89, 26.72, 25.06, 22.78, 14.21. Elem. Anal. Calcd for $C_{30}H_{43}B_2NO_4S$: C, 67.31%; H, 8.10%, N, 2.62%. Found: C, 66.47%; H, 7.73% N, 2.93%. EIMS (*m/z*): calcd for $C_{30}H_{43}B_2NO_4S$, 535.35; found, 536.

General Polymerization Procedure

All polymerization steps were carried out through the palladium(0)-catalyzed Suzuki coupling reactions. In a 50-mL flame dried two-neck flask, 1 equiv of 10-hexyl-3,7-bis (4,4,5,5-tetramethyl-1,3,2-dioxaborolan-2-yl)-10H-phenothiazine (**7**), 1 equiv of bis(bromo-4-hexyl-2-thienyl) arene (**5a**−**5c**), and $Pd(PPh_3)_4$ (1.5 mol %) were dissolved in a mixture of toluene ([monomer] = 0.5 M) and aqueous 2 M Na_2CO_3 (2:3). The solution was first put under a nitrogen atmosphere and vigorously stirred at 90−95 °C for 4−5 days. After reaction completion, an excess of bromobenzene was added to the reaction then 1 h later, excess of phenylboronic acid was added and the reaction refluxed overnight to complete the end-capping reaction. The polymer was purified by precipitation in methanol/water (10:1), filtered through 0.45 μm nylon filter and washed on Soxhlet apparatus using hexane, acetone, and chloroform. The chloroform fraction was reduced to 40−50 mL under reduced pressure, precipitated in methanol/water (10:1, 500 mL), filtered through 0.45 μm nylon filter and finally air-dried overnight.

Poly[(10-hexyl-10H-phenothiazine-3,7-ylene)-alt-(4,7-bis(4-hexylthien-2-yl)-2,1,3-benzothiadiazole) 2′,2″-diyl] (PP6DHTBT)

Dark orange solid (yield: 71%). ^{1}H-NMR (ppm, $CDCl_3$): δ 8.02 (br, 2H), 7.84 (br, 2H), 7.32 (br, 4H), 6.93 (br, 2H), 3.92 (br, 2H), 2.74 (br, 4H), 1.88 (br, 2H), 1.72 (br, 4H), 1.50 (br, 4H), 1.18-1.40 (br, 14H), 0.81−0.90 (br, 9H). Anal. Calcd C, 70.45%; H, 6.85%, N, 5.60%. Found: C, 69.78%; H, 6.97% N, 5.42%.

Poly[(10-hexyl-10H-phenothiazine-3,7-ylene)-alt-(4,7-bis(4-hexylthien-2-yl)-2,1,3- benzoselenadiazole) 2′,2″-diyl] (PP6DHTBSe)

Dark black solid (yield: 76%). ^{1}H-NMR (ppm, $CDCl_3$): δ 7.92 (br, 2H), 7.77 (br, 2H), 7.32 (br, 4H), 6.94 (br, 2H), 3.92 (br, 2H), 2.74 (br, 4H), 1.88 (br, 2H), 1.71 (br, 4H), 1.50 (br, 4H), 1.18-1.40 (br, 14H), 0.81−0.90 (br, 9H). Anal. Calcd C, 66.30%; H, 6.45%, N, 5.27%. Found: C, 64.49%; H, 6.38% N, 4.94%.

Poly[(10-hexyl-10H-phenothiazine-3,7-ylene)-alt-(4,7-bis(4-hexylthien-2-yl)-2,1,3- benzoxadiazole) 2′,2″-diyl] (PP6DHTBX)

Dark solid (yield: 69%). ^{1}H-NMR (ppm, $CDCl_3$): δ 8.00 (br, 2H), 7.53 (br, 2H), 7.30 (br, 4H), 6.91 (br, 2H), 3.89 (br, 2H), 2.69 (br, 4H), 1.88 (br, 2H), 1.69 (br, 4H), 1.48 (br, 4H), 1.18-1.40 (br, 14H), 0.81−0.90 (br, 9H). Anal. Calcd C, 71.99%; H, 7.00%, N, 5.72%. Found: C, 72.00%; H, 6.84% N, 5.75%.

RESULTS AND DISCUSSION

Synthesis and Structural Characterization

The general synthetic routes of monomers **5a–5c** and **7** are shown in Scheme 1. Synthesis of 2-(4-hexylthiophen-2-yl)-4,4,5,5-tetramethyl-1,3,2-dioxaborolane (**2**),[24(a)] 4,7-dibromo-2,1,3-benzothiadiazole (**3a**),[24(b)] 4,7-dibromo-2,1,3-benzoselenadiazole (**3b**),[23(c)] and 4,7-dibromo-2,1,3-benzoxadiazole (**3c**)[6(d)] were prepared by following the literature procedures. Hexyl-thiophene units were added to both sides of each acceptor units through the Suzuki coupling reaction between 2-(4-hexylthiophen-2-yl)-4,4,5,5-tetramethyl-1,3,2-dioxaborolane (**2**) and dibromo arenes (**3a**−**3c**) in presence of a catalyst $Pd(PPh_3)_4$. Next, these compounds were brominated with NBS to produce monomers **5a**−**5c**. The diboronic ester monomer (**7**) was prepared according to the literature method,[16(d)] that is, alkylation of phenothiazine with 1-bromohexane, followed by bromination with molecular bromine, then lithiation of dibromo compound with *n*-Buli and quenching with 2-isopropoxy-4,4,5,5-tetramethyl-1,3,2-dioxaborolane produced monomer **7**. Monomers (**5a**−**5c** and **7**) were satisfactorily characterized by ^{1}H NMR, ^{13}C NMR, MS spectroscopy, and elemental analyses. As shown in Scheme 2, three alternating polymers PP6DHTBT, PP6DHTBSe, and PP6DHTBX were prepared with the well-known Suzuki polymerization between the diboronic ester of phenothiazine (**7**)

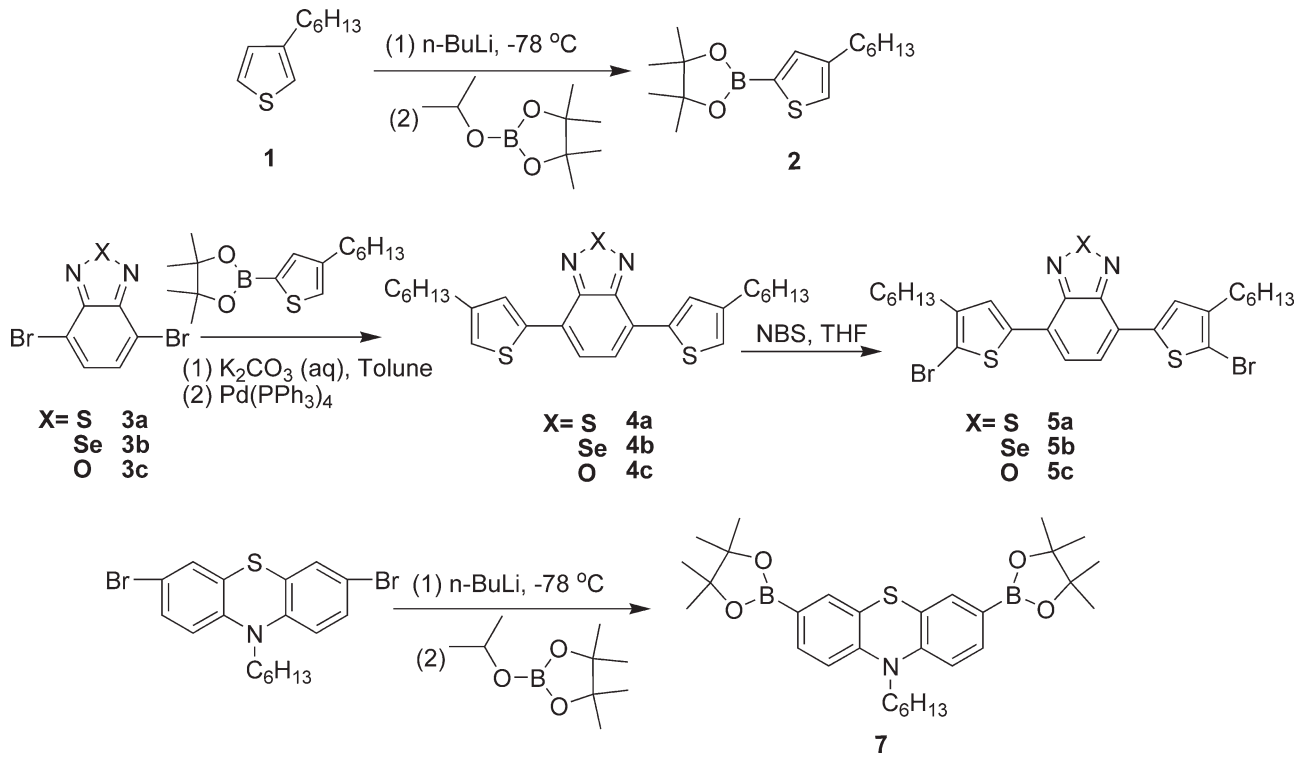

SCHEME 1 Synthetic routes of monomers (**5a**–**5c** and **7**).

and the dibromide monomers (**5a**–**5c**). The obtained polymers were further purified by washing on Soxhlet apparatus using hexane, acetone, and chloroform. The chloroform fraction was reduced to 40–50 mL under reduced pressure, precipitated in methanol, filtered through 0.45 μm nylon filters and finally dried under reduced pressure at room temperature. After purification and drying, all polymers were obtained as fibrous solids in overall good yields (69–76%). The chemical structures of the polymers were confirmed with ^{1}H-NMR and elemental analysis. The ^{1}H-NMR spectra of polymers are demonstrated in Figure 1, where the broadening signals of ^{1}H-NMR spectra in both aromatic and aliphatic regions were observed as a result of polymerization. The polymers exhibited good solubilities in common organic solvents, such as THF, chloroform, toluene, and chlorobenzene at room temperature.

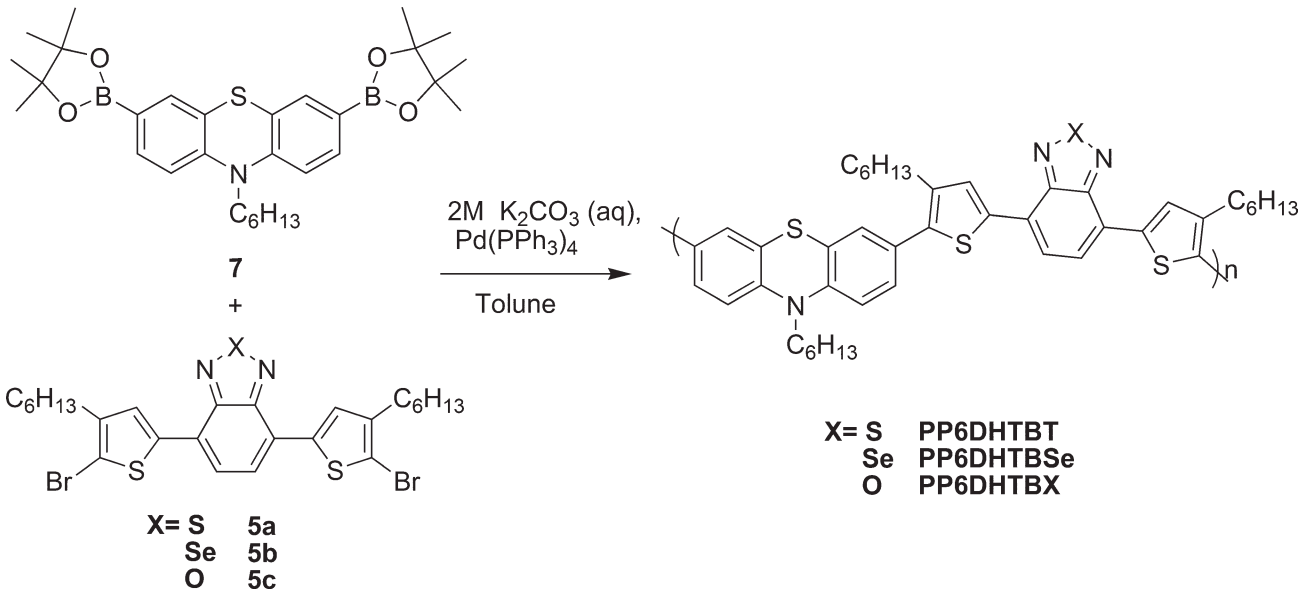

SCHEME 2 Synthetic routes of polymers (PP6DHTBT, PP6DHTBSe, and PP6DHTBX).

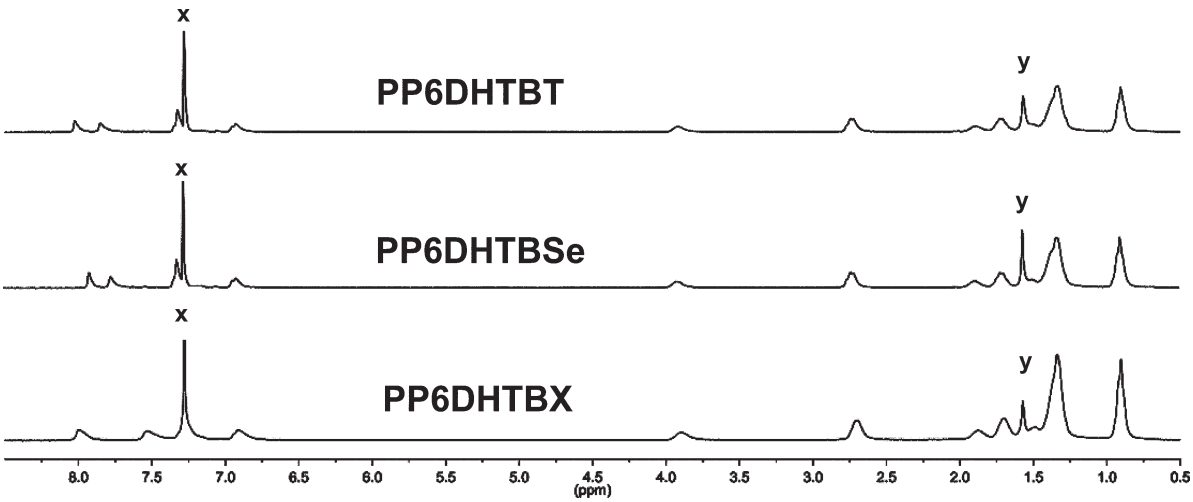

FIGURE 1 ^{1}H-NMR spectra of polymers in $CDCl_3$. Labels of x and y are $CDCl_3$ and H_2O, respectively.

The molecular weights of the polymers were determined by gel permeation chromatography (GPC) against monodisperse polystyrene standards in THF are summarized in Table 1. These results show that reasonable molecular weights were obtained in these polymers, which had number-average molecular weights (M_n) ranging 38,500−51,300 and weight-average molecular weights (M_w) ranging 64,500−101,700, respectively, with polydispersity indices (PDI = M_w/M_n) ranging 1.67−1.98. The thermal properties of the polymers determined by thermogravimetric analysis (TGA) are shown in Figure 2 and summarized in Table 1. The TGA thermograms of the polymers revealed (5% weight loss) decomposition temperatures (T_d) in the range of 401−434 °C, indicative of excellent thermal stabilities.

Optical Properties

The normalized UV−vis absorption of the synthesized polymers in dilute chlorobenzene solutions (concentration 10^{-5} M) and solid films are shown in Figure 3, and the main optical properties are listed in Table 2. The absorption spectra of polymers, that is, PP6DHTBT, PP6DHTBSe, and PP6DHTBX, exhibited two distinct broad absorption peaks. The short-wavelength absorption peaks have been attributed to a delocalized π-π^* transition in the polymer chains and long-wavelength absorption peaks attributed to a localized transition between the donor-acceptor (D-A) charge transfer states in polymer segments. The high energy transition bands situated at 300–400 nm are consistent with the reported phenothiazine homopolymers[12(b)] or phenothiazine containing copolymers.[12(c)] The low energy peaks appeared at 500−600 nm, with tailing the absorption around 700 nm are due to the ICT happening inside these phenothiazine based D-A conjugated polymers. The maximum absorption wavelengths ($\lambda_{max,abs}$) for PP6DHTBT, PP6DHTBSe, and PP6DHTBX in solutions were located at 515, 552, and 522 nm, respectively, while those in solid films at 552, 582, and 553 nm, respectively. As illustrated in Table 2, the optical band gaps (E_g^{opt}) of PP6DHTBT, PP6DHTBSe, and PP6DHTBX in solid films, which were estimated from the absorption edges of UV-vis spectra, were 1.93, 1.80, and 1.90 eV, respectively. Compared with UV−vis absorption spectra in solutions, all polymers in solid films had a red shift (30−37 nm),

TABLE 1 Molecular Weights and Thermal Properties of Polymers

Polymer	Yield (%)	M_n[a] ($\times 10^4$)	M_w[a] ($\times 10^4$)	PDI (M_w/M_n)	T_d[b] (°C)
PP6DHTBT	71	4.07	7.54	1.85	434
PP6DHTBSe	76	5.13	10.17	1.98	401
PP6DHTBX	79	3.85	6.45	1.67	417

[a] Molecular weights and polydispersity index (PDI) values were measured by GPC, using THF as an eluent, polystyrene as a standard. M_n, number average molecular weight. M_w, weight average molecular weight.
[b] Temperature (°C) at 5% weight loss measured by TGA at a heating rate of 10 °C/min under nitrogen.

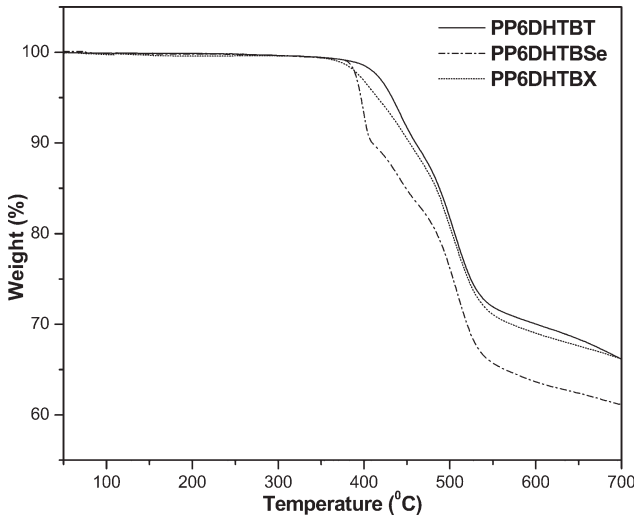

FIGURE 2 TGA thermograms of polymers.

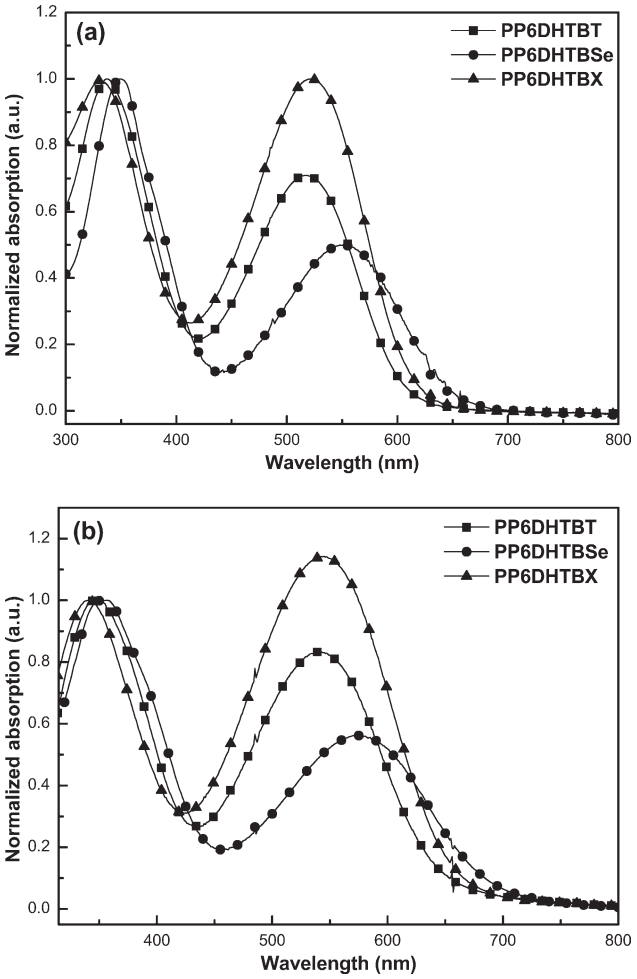

FIGURE 3 Normalized UV-vis spectra of polymers in (a) dilute chlorobenzene solutions and (b) solid films, respectively.

this could be attributed to the interchain associations and aggregations in solids. The maximum absorption wavelength ($\lambda_{max,abs}$ = 552 nm) of PP6DHTBT in solid film was red-shifted compared with that (540 nm) of its analogue F8TBT (phenothiazine units replaced with fluorene units).[25(a)] Although PP6DHTBSe bearing alkyl chains at 4-position of thiophene units revealed $\lambda_{max,abs}$ = 582 nm in solid film, which also red shifted to its fluorene-based polymer analogue bearing alkyl-chain free thiophenes, PFO-DBTSe (~570 nm).[25(b)] Since the side-chain functionalization usually cause steric hindrance to affect the coplanarity of the conjugated backbone, side-chain functionalized polymer has a blue shift in the absorption spectra compared with its side-chain free polymer analog.[26] It suggests that the phenothiazine unit possesses stronger electron-donating capability (stronger degree of delocalization and the stronger ICT) than the fluorene unit, thus to improve the effective conjugation length along the phenothiazine-based polymer backbone.[16(d)] Because of the presence of Selenium (Se) atom, which has larger size and is more electron rich than both S and O atoms, PP6DHTBSe had a more red-shifted absorption wavelength ($\lambda_{max,abs}$) compared with the other two polymers (PP6DHTBT and PP6DHTBX). Similar results were reported for the polymers containing benzoselenadiazole units,[27] where the presence of imine nitrogens in benzodiazole units can stabilize the quinoid resonance structures by the most electron rich Se atom.[27(d)]

Electrochemical Properties

The energy band structures, that is, HOMO and LUMO levels, of the polymers were investigated by cyclic voltammetry (CV) measurements to understand the charge injection processes of these polymers in their PSC devices. The cyclic voltammograms of the polymers in solid films are displayed in Figure 4 and the related CV data (formal potentials, onset potentials, HOMO and LUMO levels, and band gaps) are summarized in Table 3. Ag/AgCl was served as a reference electrode and it was calibrated by ferrocene ($E_{1/2(FC/FC^+)}$ = 0.45 eV vs. Ag/AgCl). The HOMO and LUMO energy levels were estimated by the oxidation and reduction potentials from the reference energy level of ferrocene (4.8 eV below the vacuum level) according to the following equation[28]: $E_{HOMO}/E_{LUMO} = [-(E_{onset} - E_{onset(FC/FC^+ \text{ vs. } Ag/Ag^+)}) - 4.8]$ eV, where 4.8 eV is the energy level of ferrocene below the vacuum level and $E_{onset(FC/FC^+ \text{ vs. } Ag/Ag^+)}$ = 0.45 eV. All polymers exhibited one quasi-reversible *p*-doping/dedoping (oxidation/rereduction) process at positive potentials and one quasi-reversible or reversible *n*-doping/dedoping (reduction/reoxidation) process at negative potentials, which are good signs of high structural stability in the charged state.

The HOMO levels were in the range of −5.38 to −5.47 eV, which were estimated from the onset oxidation potentials ($E_{ox/onset}$) of polymers (1.03−1.12 V). The LUMO levels were

TABLE 2 Optical Properties of Polymers

	Solution[a]			Solid Film[b]		
Polymer	$\lambda_{max,abs}$ (nm)	λ_{edge} (nm)	E_g^{opt} (eV)[c]	$\lambda_{max,abs}$ (nm)	λ_{edge} (nm)	E_g^{opt} (eV)[c]
PP6DHTBT	337,515	607	2.04	347,552	642	1.93
PP6DHTBSe	349,552	656	1.89	358,582	689	1.80
PP6DHTBX	330,522	610	2.03	341,553	652	1.90

[a] In chlorobenzene dilute solution.
[b] Spin coated from chlorobenzene solution.
[c] The optical bandgap was obtained from the equation $E_g = 1240/\lambda_{edge}$.

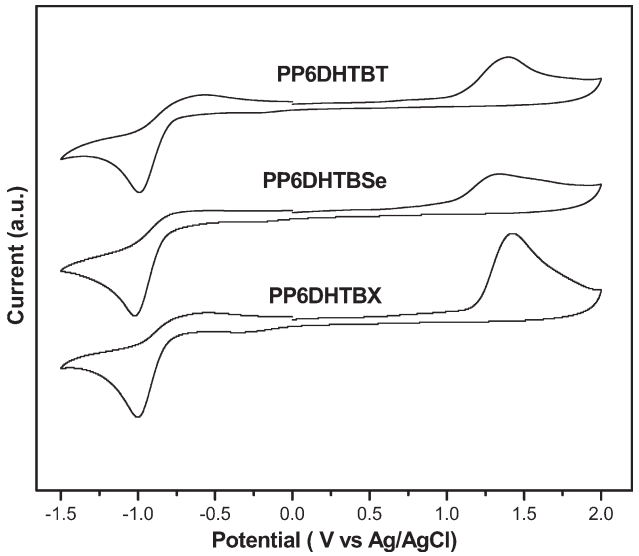

FIGURE 4 Cyclic voltammograms of polymers.

in the range of −3.47 to −3.60 eV, which were estimated from the onset reduction potentials ($E_{red/onset}$) of polymers (−0.75 to −0.88 V). As all HOMO levels were below the air oxidation threshold (ca. −5.27 eV or 0.57 V vs. SCE),[29] the polymers should show good air stabilities. More importantly, the introduction of phenothiazine unit in the PP6DHTBT polymer backbone decreases the energy band gap in contrast to its fluorene analog F8TBT,[25(a)] which may be due to the presence of electron-rich sulfur and nitrogen heteroatoms of the phenothiazine unit that renders the resulting conjugated backbone more electron-rich.[16(d)] On the other hand, the LUMO energy levels are clearly affected by the electron-deficient centers of the benzodiazole comonomers, stronger electron-deficient units resulting in lower LUMO energy levels. It has been found that the band gaps of these polymers were affected due to stronger ICT interactions between the donor phenothiazine unit and acceptor benzodiazole units. It is worth also noting that the band-gap values directly measured by CV (E_g^{ec} between 1.83 and 1.95 eV) and the optical band-gap values estimated from UV–vis spectra (E_g^{opt} between 1.80 and 1.93 eV) are relatively in good agreement. All these electrochemical characteristics are within the desirable range for the ideal polymers to be utilized in the organic photovoltaic applications.

Photovoltaic Properties

To investigate the potential use of polymers PP6DHTBT, PP6DHTBSe, and PP6DHTBX in PSCs, the bulk heterojunction (BHJ) solar cell devices comprising of these polymers as electron donors and fullerene derivatives ($PC_{61}BM$ or $PC_{71}BM$) as an electron acceptor in their active layer were fabricated with a structure of ITO/PEDOT:PSS (30 nm)/polymer:PCBM blend (∼80 nm)/Ca (30 nm)/Al (100 nm). The blended solutions were prepared with polymers and $PC_{61}BM$ in a weight ratio of 1:1 (w/w) initially, and later the active layer compositions were modified with various weight ratios for the previous optimum polymer with $PC_{71}BM$. The current density (J) versus voltage (V) curves of the PSCs are shown in Figure 5; the open circuit voltage (V_{oc}), short circuit current density (J_{sc}), fill factor (FF), and the PCE values of the devices are summarized in Table 4. In BHJ solar cell devices, V_{oc} is determined by the difference between HOMO level of the electron donor polymer and LUMO level of the electron acceptor material (PCBM).[7(a)] Because of negligible differences in HOMO levels of all polymers ((−5.38) − (−5.47) eV), there were minor variations in V_{oc} values (0.69−0.65 V). With the similar V_{oc} values and fill factor (29.1−32.1%) in the devices containing the polymers blended with $PC_{61}BM$ in a weight ratio of 1:1 (w/w), it was evident that due to the major variations of the J_{sc} values (1.92, 1.43, and 1.24 mA/cm^2) in polymers PP6DHTBT, PP6DHTBSe, and PP6DHTBX, they are crucially affected to have the PCE values of 0.41, 0.28, and 0.25, respectively. Among these PSC devices containing polymers, the best performance was the PSC device containing PP6DHTBT:$PC_{61}BM$ (1:1 w/w) with a highest PCE value of 0.41%, V_{oc} = 0.67 V, J_{sc} = 1.92 mA/cm^2, and FF = 32.1%.

Since the best performance of PSC device was observed in the previous optimum polymer blend PP6DHTBT:$PC_{61}BM$ (1:1 wt %) as an active layer, the PSC devices as a function of polymer blends PP6DHTBT:$PC_{71}BM$ in various weight compositions (1:1, 1:3, and 1:4 w/w) were fabricated owing

TABLE 3 Electrochemical Properties of Polymers[a]

	Oxidation Potential (V vs. Ag/Ag$^+$)		Reduction Potential (V vs. Ag/Ag$^+$)		Energy Level[b] (eV)		Band Gap eV)	
Polymer	$E_{ox/onset}$[c]	$E_{ox/o}$[d]	$E_{red/onset}$[c]	$E_{red/o}$[d]	HOMO	LUMO	E_g^{ec}	E_g^{opt}
PP6DHTBT	1.07	1.36	−0.88	−0.97	−5.42	−3.47	1.95	1.93
PP6DHTBSe	1.03	1.31	−0.80	−1.01	−5.38	−3.55	1.83	1.80
PP6DHTBX	1.12	1.40	−0.75	−0.99	−5.47	−3.60	1.87	1.90

[a] Reduction and oxidation potentials measured by cyclic voltammetry in solid films.
[b] E_{HOMO}/E_{LUMO} = [−(E_{onset} − 0.45) − 4.8] eV, where 0.45 V is the value for ferrocene versus Ag/Ag$^+$ and 4.8 eV is the energy level of ferrocene below the vacuum.
[c] Onset oxidation and reduction potentials.
[d] Formal oxidation and reduction potentials.

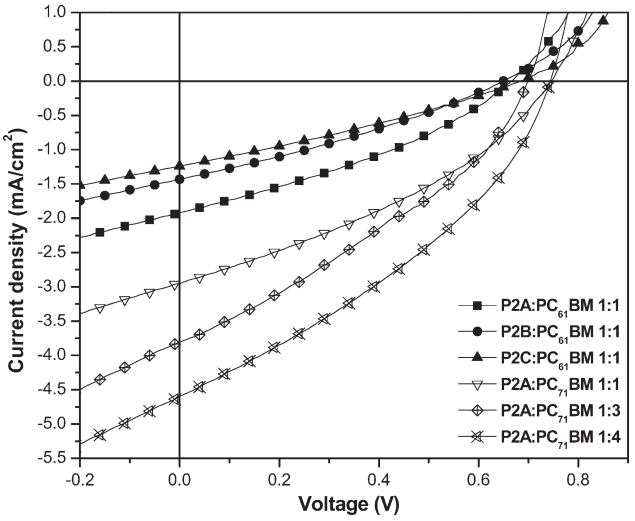

FIGURE 5 Current–voltage curves of PSCs using polymer:PCBM blends under the illumination of AM 1.5G, 100 mW/cm^2.

to a broader absorption and a higher absorption coefficient of $PC_{71}BM$ than $PC_{61}BM$.[1(d)] The absorption spectra of the polymer blends PP6DHTBT:$PC_{71}BM$ (1:1, 1:3, and 1:4 w/w) prepared under the same conditions as the process of device fabrication are demonstrated in Figure 6(a). The current–voltage characteristics of these devices are also shown in Figure 5, and their related photovoltaic properties are illustrated in Table 4. The optimum photovoltaic performance with the maximum PCE value of 1.20% (V_{oc} = 0.75 V, J_{sc} = 4.60 mA/cm^2, and FF = 35.0%) was obtained in the PSC device having a weight ratio of PP6DHTBT:$PC_{71}BM$ = 1:4. Using lower weight ratios of PCBM in blended polymer PP6DHTBT:$PC_{71}BM$ (1:1 and 1:3 w/w) led to reductions in the J_{sc} values due to the inefficient charge separation and electron transporting properties, resulting in the lower PCE results.[30]

The V_{oc} values observed in PP6DHTBT:$PC_{71}BM$ solar cells were fairly stable (0.73–0.75 V) in all polymer blend compositions (1:1–1:4 w/w) with $PC_{71}BM$ (Table 4), which are

TABLE 4 Photovoltaic Properties of Polymer Solar Cell Devices with the Configuration of ITO/PEDOT:PSS/Polymer:PCBM/Ca/Al[a]

Polymer	Polymer/PCBM (w/w)	V_{oc} (V)	J_{sc} (mA/cm^2)	FF (%)	PCE (%)
PP6DHTBT	1:1 (C61)	0.67	1.92	32.1	0.41
PP6DHTBSe	1:1 (C61)	0.65	1.43	30.5	0.28
PP6DHTBX	1:1 (C61)	0.69	1.24	29.1	0.25
PP6DHTBT	1:1 (C71)	0.73	2.95	34.0	0.74
PP6DHTBT	1:3 (C71)	0.73	3.80	33.1	0.88
PP6DHTBT	1:4 (C71)	0.75	4.60	35.0	1.20

[a] Measured under AM 1.5 irradiation, 100 mW/cm^2.

comparable to that of some of donor acceptor polymer:fullerene BHJ solar cells.[17–22] The EQE curves of the PSC devices are also plotted in Figure 6(b) to compare with the absorption spectra of the polymer blends PP6DHTBT:$PC_{71}BM$ shown in Figure 6(a). It is apparent that the PSC devices exhibited a very broad response range covering from 400 to 700 nm, where the EQEs were within 30%. The main reason for the low EQE values of the PSC devices are due to the limited absorbances of the active layer as shown in Figure 6(a). In BHJ solar cell devices, the absorptions of the long wavelength region are contributed by the polymers, and the absorptions in the short wavelength region are mainly from $PC_{71}BM$. However, the peak values of the absorbances in the long wavelength region are only 0.17–0.30, so it means that

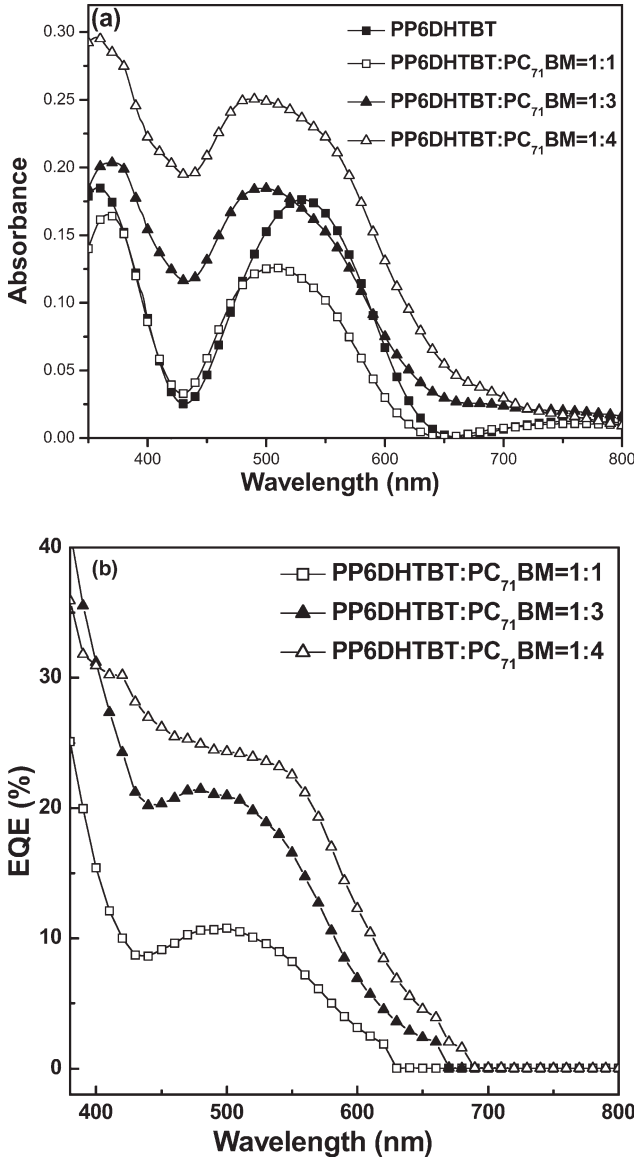

FIGURE 6 (a) Absorbance spectra of PP6DHTBT:$PC_{71}BM$ thin films measured from the solar cell devices by using an ITO/PEDOT substrate as a reference. (b) EQE of PP6DHTBT:$PC_{71}BM$ solar cells.

only some portions of light were absorbed in the PSC devices, which might be due to the small thickness of the active layer (~80 nm).

Carrier transport properties, including hole and electron mobilities of PP6DHTBT:$PC_{71}BM$ (1:4 wt %) were evaluated by fabricating the hole- and electron-only devices. The devices were prepared following the same procedure as the fabrication of BHJ devices, except that Ca was replaced with MoO_3 (Φ = 5.3 eV) in the hole-only devices, and the PEDOT:PSS layer was replaced with Cs_2CO_3 (Φ = 2.9 eV) for the electron-only devices. The electron and hole mobilities were determined precisely by fitting the plots of the dark current versus voltage (*J–V*) curves for single carrier devices to the space charge limited current (SCLC) model. The dark current is given by $J = 9\varepsilon_0\varepsilon_r\mu V^2/8L^3$, where $\varepsilon_0\varepsilon_r$ is the permittivity of the polymer, μ is the carrier mobility, and L is the device thickness. The hole and electron mobilities of PP6DHTBT:$PC_{71}BM$ (1:4 wt %) are 3.68×10^{-9} cm^2/Vs and 1.76×10^{-8} cm^2/Vs, respectively. The electron mobility was much higher (i.e., ca. 1 order of magnitude) than the hole mobility, resulting in an imbalance in the hole and electron transport in the blended polymer film. Because of the poor hole mobility and the imbalance of the hole and electron transport in the blended polymer film, the device was limited to have a low FF value, which could be another reason for the lower PCE value.[31] From the AFM images of PP6DHTBT:$PC_{71}BM$ with various weight ratios (Fig. 7), we observed that the roughness is increased from 0.67 nm (with PCE = 0.74%) to 1.48 nm (with PCE = 0.88%) and 2.60 nm (with PCE = 1.20%) as the weight ratio of PP6DHTBT:$PC_{71}BM$ changed from 1:1 to 1:3 and 1:4 w/w ratio, respectively. Therefore, we can summarize that the increased PCE value caused by a higher content of $PC_{71}BM$ in the polymer blend of PP6DHTBT:$PC_{71}BM$ = 1:4 w/w was induced by the larger roughness in the polymer blend. In addition, the optimum PSC device (without annealing, PCE = 1.20%) containing polymer blend of PP6DHTBT:$PC_{71}BM$ = 1:4 (w/w) was further investigated for the thermal annealing effects. As shown in Table 5, the PCE values of 1.14, 1.05, and 0.86% were obtained at the thermal annealing (20 min) of 50, 100, and 150 °C, respectively. Finally, the thermal annealing effects were proven to have no substantial increase on the solar cell device performance.

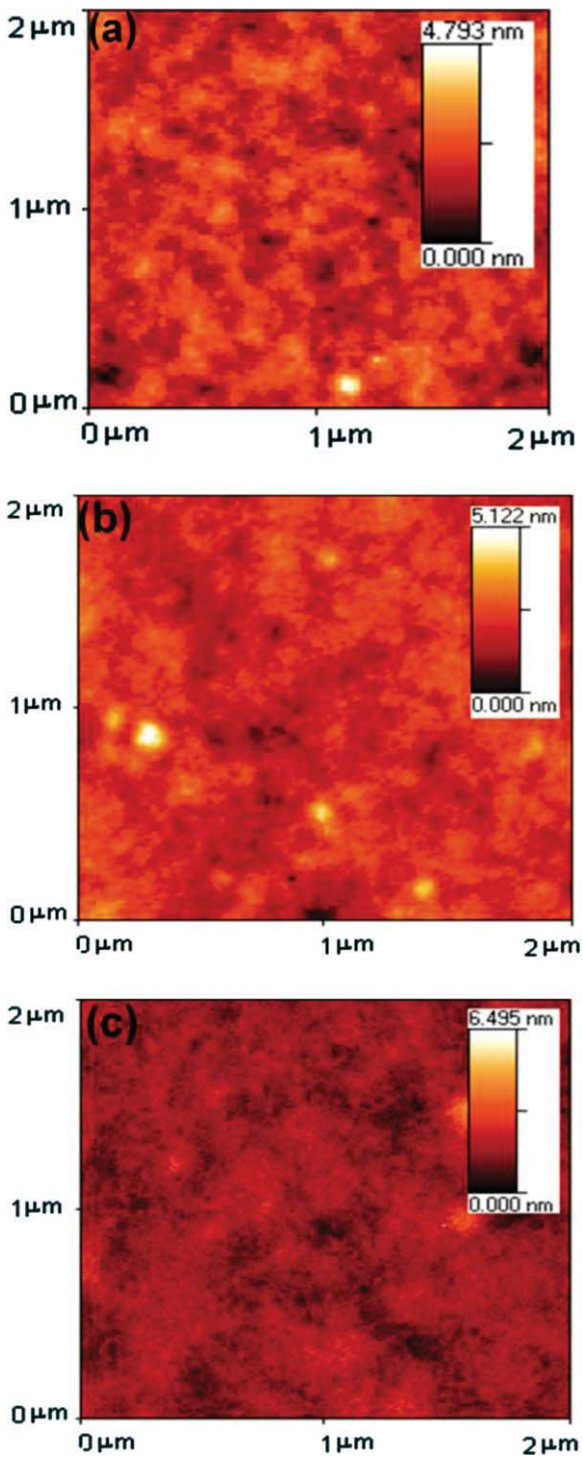

FIGURE 7 AFM images of PP6DHTBT: $PC_{71}BM$ blend films. (a) 1:1 (w/w), (b) 1:3 (w/w), and (c) 1:4 (w/w) ratios.

TABLE 5 Annealing Effects on Polymer Solar Cell Device Containing PP6DHTBT:$PC_{71}BM$ (1:4 wt%)

Annealing Temperature (°C)	V_{oc} (V)	J_{sc} (mA/cm^2)	FF (%)	PCE (%)
50	0.73	4.99	31.3	1.14
100	0.74	4.37	32.6	1.05
150	0.67	4.09	31.2	0.86

CONCLUSIONS

In summary, a series of new LBG polymers containing the phenothiazine unit as an electron donor conjugated with various benzodiazole acceptors via hexyl-thiophene linkers were synthesized and characterized. These polymers show strong absorptions in the range of 300–700 nm and have ideal ranges of HOMO and LUMO levels (with optical bandgaps of 1.80–1.93 eV). Bulk heterojunction PSCs were fabricated from the polymer blends consisting of these LBG polymers

(PP6DHTBT, PP6DHTBSe, and PP6DHTBX) as an electron donor and $PC_{61}BM$/$PC_{71}BM$ as an electron acceptor. With the similar V_{oc} values and fill factor in the PSC devices containing the polymers blended with $PC_{61}BM$ in a weight ratio of 1:1 (w/w), it was found that due to the major variations of the J_{sc} values (1.92, 1.43, and 1.24 mA/cm^2) in polymers PP6DHTBT, PP6DHTBSe, and PP6DHTBX, they are crucially affected to have the PCE values of 0.41, 0.28, and 0.25, respectively. The PSC device containing a polymer blend of PP6DHTBT:$PC_{71}BM$ (1:4 wt %) exhibited the best device performance with a PCE value of 1.20%, an open-circuit voltage (V_{oc}) of 0.75 V, a short-circuit current (J_{sc}) of 4.60 mA/cm^2, and a fill factor (FF) of 0.35. The optimization of photovoltaic properties in the PSC devices containing polymer blends PP6DHTBT:$PC_{71}BM$ can be adjusted by the morphology variations with different weight ratios of $PC_{71}BM$, which were observed to have higher roughnesses with larger $PC_{71}BM$ contents, and thus to substantially increase the PCE values of the PSC devices. Finally, this study revealed that these new phenothiazine-based LBG polymers will have potential applications for the flexible electronic devices.

We are grateful to the National Center for High-performance Computing for computer time and facilities. The financial supports of this project provided by the National Science Council of Taiwan (ROC) through NSC 97-2113*M*-009-006-MY2, National Chiao Tung University through 97W807, and Energy and Environmental Laboratories (charged by Chang-Chung Yang) in Industrial Technology Research Institute (ITRI) are acknowledged.

REFERENCES AND NOTES

1 (a) Brabec, C. J.; Sariciftci, N. S.; Hummelen, J. C. Adv Funct Mater 2001, 11, 15–26; (b) Günes, S.; Neugebauer, H.; Sariciftci, N. S. Chem Rev 2007, 107, 1324–1338; (c) Dennler, G.; Scharber, M.; Brabec, C. J. Adv Mater 2009, 21, 1323–1338; (d) Thompson, B. C.; Fréchet, J. M. J. Angew Chem Int Ed Engl 2008, 47, 58–77; (e) Hoppe, H.; Sariciftci, N. S. J Mater Chem 2006, 16, 45–61; (f) Bundgaard, E.; Krebs, F. C. Sol Energy Mater Sol Cells 2007, 91, 954–985; (g) Kroon, R.; Lenes, M.; Hummelen, J. C. Polym Rev 2008, 48, 531–582.

2 (a) Li, G.; Shrotriya, V.; Huang, J.; Yao, Y.; Moriarty, T.; Emery, K.; Yang, Y. Nat Mater 2005, 4, 864–868; (b) Ma, W. L.; Yang, C. Y.; Gong, X.; Lee, K.; Heeger, A. J Adv Funct Mater 2005, 15, 1617–1622; (c) Li, G.; Shrotriya, V.; Yao, Y.; Yang, Y. J Appl Phys 2005, 98, 043704.

3 (a) Liang, Y. Y.; Wu, Y.; Feng, D. Q.; Tsai, S. T.; Son, H. J.; Li, G.; Yu, L. P. J Am Chem Soc 2009, 131, 56–57; (b) Liang, Y. Y.; Feng, D. Q.; Wu, Y.; Tsai, S. T.; Li, G.; Ray, C.; Yu, L. P. J Am Chem Soc 2009, 131, 7792; (c) Park, S. H.; Roy, A.; Beaupre, S.; Cho, S.; Coates, N.; Moon, J. S.; Moses, D.; Leclerc, M.; Lee, K.; Heeger, A. J. Nat Photonics 2009, 3, 297–303; (d) Hou, J. H.; Chen, H. Y.; Zhang, S. Q.; Chen, R. I.; Yang, Y.; Wu, Y.; Li, G. J Am Chem Soc 2009, 131, 15586–15587; (e) Chen, H.-Y.; Hou, J.; Zhang, S.; Liang, Y.; Yang, G.; Yang, Y.; Yu, L.; Wu, L.; Li, G. Nat Photonics 2009, 3, 649–653.

4 (a) Li, G.; Yao, Y.; Yang, H.; Shrotriya, V.; Yang, G.; Yang, Y. Adv Funct Mater 2007, 17, 1636–1644; (b) Li, G.; Shrotriya, V.; Yao, Y.; Huang, J. S.; Yang, Y. J Mater Chem 2007, 17, 3126–3140; (c) Nguyen, L H.; Hoppe, H.; Erb, T.; Gunes, S.; Gobsch, G.; Sariciftci, N. S. Adv Funct Mater 2007, 17, 1071–1078; (d) Guo, X. G.; Kim, F. S.; Jenekhe, S. A.; Watson, M. D. W. J Am Chem Soc 2009, 131, 7206–7207; (e) Hsu, S. L. C.; Lin, Y. C.; Lee, R. F.; Sivakumar, C.; Chen, J. S.; Chou, W. Y. J Polym Sci Part A: Polym Chem 2009, 47, 5336–5343; (f) Zhang, S. M.; Fan, H. J.; Liu, Y.; Zhao, G. J.; Li, Q. K.; Li, Y. F.; Zhan, X. W. J Polym Sci Part A: Polym Chem 2009, 47, 2843–2852.

5 (a) Xin, H.; Kim, F. S.; Jenekhe, S. A. J Am Chem Soc 2008, 130, 5424–5425; (b) Chang, Y. T.; Hsu, S. L.; Chen, G. Y.; Su, M. H.; Singh, T. A.; Diau, E. W. G.; Wei, K. H. Adv Funct Mater 2008, 18, 2356–2365; (c) Xin, H.; Ren, G.; Kim, F. S.; Jenekhe, S. A. Chem Mater 2008, 20, 6199–6207; (d) Yao, Y.; Hou, J. H.; Xu, Z. X.; Li, G.; Yang, Y. Adv Funct Mater 2008, 18, 1783–1789; (e) Peet, J.; Kim, J. Y.; Coates, N. E.; Ma, W. L.; Moses, D.; Heeger, A. J.; Bazan, G. C. Nature Mater 2007, 6, 497–500.

6 (a) Zhu, Z. G.; Waller, D.; Gaudiana, R.; Morana, M.; Muhlbacher, D.; Scharber, M.; Brabec, C. Macromolecules 2007, 40, 1981–1986; (b) Zhang, F. L.; Bijleveld, J.; Perzon, E.; Tvingstedt, K.; Barrau, S.; Inganas, O.; Andersson, M. R. J Mater Chem 2008, 18, 5468–5474; (c) Li, Y. F.; Zou, Y. P. Adv Mater 2008, 20, 2952–2958; (d) Blouin, N.; Michaud, A.; Gendron, D.; Wakim, S.; Blair, E.; Plesu, R. N.; Bellette, M.; Durocher, G.; Tao, Y.; Leclerc, M. J Am Chem Soc 2008, 130, 732–742; (e) Soci, C.; Hwang, I.-W.; Moses, D.; Zhu, Z.; Waller, D.; Gaudiana, R.; Brabec, C. J.; Heeger, A. J Adv Funct Mater 2007, 17, 632–636; (f) Kim, J. Y.; Lee, K.; Coates, N. E.; Moses, D.; Nyuyen, T.-Q.; Heeger, A. J. Science 2007, 317, 222–225; (g) Bundgaard, E.; Krebs, F. C. Sol Energy Mater Sol Cells 2007, 91, 1019–1025; (h) Chen, C. P.; Chan, S. H.; Chao, T. C.; Ting, C.; Ko, B. T. J Am Chem Soc 2008, 130, 12828–12833.

7 (a) Scharber, M. C.; Muehlbacher, D.; Koppe, M.; Denk, P.; Waldauf, C.; Heeger A. J.; Brabec, C. J. Adv Mater 2006, 18, 789–793; (b) Zhang, F. L.; Mammo, W. L.; Anderson, M.; Admassie, S. M.; Andersson, R.; Inganas, O. Adv Mater 2006, 18, 2169–2173; (c) Wienk, M. M.; Turbiez, W.; Gilot, G.; Janssen, R. A. Adv Mater 2008, 20, 2556–2560; (d) Lee, S. K.; Cho, N. S.; Cho, S.; Moon, S. J.; Lee, J. K., Bazan, G. C. J Polym Sci Part A: Polym Chem 2009, 47, 6873–6882; (e) Wan, M. X.; Wu, W. P.; Sang, G. Y.; Zou, Y. P.; Liu, Y. Q.; Li, Y. F. J Polym Sci Part A: Polym Chem 2009, 47, 4028–4036.

8 (a) Bre'das, J. L. J Chem Phys 1985, 82, 3808–381; (b) Roncali, J. Chem Rev 1997, 97, 173–206.

9 Blom, P. W. M.; Mihailetchi, V. D.; Koster, L. J. A.; Markov, D. E. Adv Mater 2007, 19, 1551–1566.

10 Bredas, J.-L.; Beljonne, D.; Coropceanu, V.; Cornil, J. Chem Rev 2004, 104, 4971–5003.

11 (a) Jenekhe, S. A.; Lu, L.; Alam, M. M. Macromolecules 2001, 34, 7315–7324; (b) Bates, W. D.; Chen, P. Y.; Dattelbaum, D. M.; Jones, W. E.; Meyer, T. J. J Phys Chem A 1999, 103, 5227–5231; (c) Pfennig, B. W.; Chen, P. Y.; Meyer, T. J. Inorg Chem 1996, 35, 2898–2901.

12 (a) Cho, N. S.; Park, J. H.; Lee, S. K.; Lee, J.-H.; Shim, H.-K.; Park, M.-J.; Hwang, D.-H.; Jung, B.-J. Macromolecules 2006,

39, 177–183; (b) Hwang, D.-H.; Kim, S.-K.; Park, M.-J.; Lee, J.-H.; Koo, B.-W.; Kang, I.-N.; Kim, S.-H.; Zyung, T. Chem Mater 2004, 16, 1298–1303; (c) Park, M. J.; Lee, J.; Jung, I. H.; Park, J. H.; Hwang, D. H.; Shim, H. K. Macromolecules 2008, 41, 9643–9649.

13 (a) Lai, R. Y.; Kong, X.; Jenekhe, S. A.; Bard, A. J. J Am Chem Soc 2003, 125, 12631–12639; (b) Fungo, F.; Jenekhe, S. A.; Bard, A. J Chem Mater 2003, 15, 1264–1272; (c) Sun, D.; Rosokha, S. V.; Koich, J. K. J Am Chem Soc 2004, 126, 1388–1401.

14 Zou, Y.; Wu, W.; Sang, G.; Yang, Y.; Liu, Y.; Li, Y. Macromolecules 2007, 40, 7231–7237.

15 Kong, X.; Kulkarni, A. P.; Jenekhe, S. A. Macromolecules 2003, 36, 8992–8999.

16 (a) Tang, W. H.; Kietzke, T.; Vemulamada, P.; Chen, Z. K. J Polym Sci Part A: Polym Chem 2007, 45, 5266–5276; (b) Sang, G. Y.; Zou, Y. P.; Li, Y. F. J Phys Chem C 2008, 112, 12058–12064; (c) Wong, W. Y.; Chow, W. C.; Cheung, K. Y.; Fung, M. K.; Djurisic, A. B.; Chan, W. K. J Organometallic Chem 2009, 694, 2717–2726; (d) Li, Y. W.; Xue, L. L.; Li, H.; Li, Z. F.; Xu, B.; Wen, S. P.; Tian, W. J. Macromolecules 2009, 42, 4491–4499; (e) Li, K. C.; Hsu, Y. C.; Lin, J. T.; Yang, C. C.; Wei, K. H.; Lin, H. C. J Polym Sci Part A: Polym Chem 2008, 46, 4285–4304; (f) Huang, J. H.; Li, K. C.; Wei, H. Y.; Chen, P. Y.; Lin, L. Y.; Kekuda, D.; Lin, H. C.; Ho, K. C.; Chu, C. W. Org Electronics 2009, 10, 1109–1115.

17 (a) Svensson, M.; Zhang, F. L.; Veenstra, S. C.; Verhees, W. J. H.; Hummelen, J. C.; Kroon, J. M.; Inganas, O.; Andersson, M. R. Adv Mater 2003, 15, 988–991; (b) Slooff, L. H.; Veenstra, S. C.; Kroon, J. M.; Moet, D. J. D.; Sweelssen, J.; Koetse, M. M. Appl Phys Lett 2007, 90, 143506; (c) Shi, C.; Yao, Y.; Yang, Y.; Pei, Q. J Am Chem Soc 2006, 128, 8980–8986; (d) Wang, E. G.; Wang, M.; Wang, L.; Duan, C. H.; Zhang, J.; Cai, W. Z.; He, C.; Wu, H. B.; Cao, Y. Macromolecules 2009, 42, 4410–4415.

18 (a) Boudreault, P. T.; Michaud, A.; Leclerc, M. Macromol Rapid Commun 2007, 28, 2176–2179; (b) Wang, E. G.; Wang, L.; Lan, L. F.; Luo, C.; Zhuang, W. L.; Peng, J. B.; Cao, Y. Appl Phys Lett 2008, 92, 033307.

19 Blouin, N.; Michaud, A.; Leclerc, M. Adv Mater 2007, 19, 2295–2300.

20 (a) Hou, J. H.; Chen, H. Y.; Zhang, S. Q.; Li, G.; Yang, Y. J. Am Chem Soc 2008, 130, 16144–16145; (b) Liao, L.; Dai, L. M.; Smith, A.; Durstock, M.; Lu, J. P.; Ding, J. F.; Tao, Y. Macromolecules 2007, 40, 9406–9412.

21 (a) Muhlbacher, D.; Scharber, M.; Morana, M.; Zhu, Z.; Waller, D.; Gaudiana, R.; Brabec, C. Adv Mater 2006, 18, 2884–2889; (b) Moule, A. J.; Tsami, A.; Bunnagel, T. W.; Forster, M.; Kronenberg, N. M.; Scharber, M.; Koppe, M.; Morana, M.; Brabec, C. J.; Meerholz, K.; Scherf, U. Chem Mater 2008, 20, 4045–4050.

22 Yue, W.; Zhao, Y.; Shao, S.; Tian, H.; Xie, Z.; Geng, Y.; Wang, F. J Mater Chem 2009, 19, 2199–2206.

23 (a) Zhang, F.; Perzon, E.; Wang, X.; Mammo, W.; Andersson, M. R.; Inganas, O. Adv Funct Mater 2005, 15, 745–750; (b) Ashraf, R. S.; Hoppe, H.; Shahid, M.; Gobsch, G.; Sensfuss, S.; Klemm, E. J Polym Sci Part A: Polym Chem 2006, 44, 6952–6961; (c) Wang, F.; Luo, J.; Yang, K.; Chen, J.; Huang, F.; Cao, Y. Macromolecules 2005, 38, 2253–2260.

24 (a) Gautrot, J. E.; Hodge, P.; Cupertio, D.; Helliwell, M.; New J Chem 2007, 31, 1585–1593; (b) Tsami, A.; Bunnagel, T. W.; Farrell, T.; Scharber, M.; Choulis, S. A.; Brabec, C. J.; Scherf, U. J Mater Chem 2007, 17, 1353–1355.

25 (a) McNeill, C. R.; Halls, J. J. M.; Wilson, R.; Whiting, G. L.; Berkebile, S.; Ramsey, M. G.; Friend, R. H.; Greenham, N. C. Adv Funct Mater 2008, 18, 2309–2321; (b) Iuo, J.; Hou, Q.; Chen, J.; Cao, Y. Synth Metals 2006, 156, 470–475.

26 (a) Cho, S.; Seo, J. H.; Kim, S. H.; Song, S.; Jin, Y.; Lee, K.; Suh, H.; Heeger, A. J. Appl Phys Lett 2008, 93, 263301; (b) Zhou, H. X.; Yang, L. Q.; Xiao, S. Q.; Liu, S. B.; You, W. Macromolecules 2010, 43, 811–820; (c) Zhang, S. M.; Guo, Y. L.; Fan, H. J.; Liu, Y.; Chen, H. Y.; Yang, G. W.; Zhan, X. W.; Liu, Y. Q.; Li, Y. F.; Yang, Y. J Polym Sci Part A: Polym Chem 2009, 47, 5498–5508; (d) Song, S.; Jin, Y.; Kim, S. H.; Moon, J.; Kim, K.; Kim, J. Y.; Park, S. H.; Lee, K.; Suh, H. Macromolecules 2008, 41, 7296–7305.

27 (a) Yang, R.; Tian, R.; Hou, Q.; Yang, W.; Cao, Y. Macromolecules 2003, 36, 7453–7460; (b) Jung, I. H.; Kim, H.; Park, M. J.; Kim, B.; Park, J. H.; Jeong, E.; Woo, H. Y.; Yoo, S.; Shim, H. K. J Polym Sci Part A: Polym Chem 2010, 48, 1423–1432; (c) Huang, F.; Hou, L.; Shen, H.; Yang, R.; Hou, Q.; Cao, Y. J Polym Sci Part A: Polym Chem 2006, 44, 2521–2532; (d) Ono, K.; Tanaka, S.; Yamashita, Y. Angew Chem Int Ed 1994, 33, 1977–1980.

28 (a) Chen, Y. Y.; Tao, Y. T.; Lin, H. C. Macromolecules 2006, 39, 8559–8566; (b) Li, K. C.; Hsu, Y. C.; Lin, J. T.; Yang, C.; Wei, K. H.; Lin, H. C. J Polym Sci Part A: Polym Chem 2009, 47, 2073–2092.

29 de Leeuw, D. M.; Simenon, M. M. J.; Brown, A. R.; Einhard, R. E. F. Synth Met 1997, 87, 53–59.

30 Baek, N. S.; Hau, S. K.; Yip, H. L.; Acton, O.; Chen, K. S.; Jen, A. K. Y. Chem Mater 2008, 20, 5734–5736.

31 Hou, J.; Chen, T. L.; Zhang, S.; Chen, H.-Y.; Yang, Y. J Phys Chem C 2009, 113, 1601–1605.